X-620-72-40
PREPRINT

X- 65826

INFRARED SPECTROSCOPY EXPERIMENT ON MARINER 9

PRELIMINARY RESULTS

FEBRUARY 1972

GSFC
GODDARD SPACE FLIGHT CENTER
GREENBELT, MARYLAND

(NASA-TM-X-65826) INFRARED SPECTROSCOPY EXPERIMENT ON MARINER 9: PRELIMINARY RESULTS R.A. Hanel, et al (NASA) Feb. 1972 12 p CSCL 03A
N72-17911
Unclas
G3/30 17333

X-620-72-40

INFRARED SPECTROSCOPY EXPERIMENT ON MARINER 9

PRELIMINARY RESULTS

R. A. Hanel, B. J. Conrath, W. A. Hovis, V. G. Kunde,
P. D. Lowman, J. C. Pearl, C. Prabhakara, B. Schlachman
Goddard Space Flight Center
Greenbelt, Maryland 20771

G. Levin
Biospherics Incorporated
4928 Wyaconda Road
Rockville, Maryland 20853

February 1972

GODDARD SPACE FLIGHT CENTER
Greenbelt, Maryland

INFRARED SPECTROSCOPY EXPERIMENT ON MARINER 9

PRELIMINARY RESULTS

ABSTRACT

The Mariner 9 infrared spectroscopy experiment has provided good quality spectra of many areas of Mars, predominantly in the southern hemisphere. Large portions of the thermal emission spectra are significantly affected by dust with a silicon oxide content approximately corresponding to that of an intermediate igneous rock, implying that Mars has undergone a substantial geochemical differentiation. Derived temperature profiles indicate a warm daytime upper atmosphere with a strong warming over the south polar cap. Atmoshperic water vapor is clearly observed over the south polar area and less strongly over other regions.

PRECEDING PAGE BLANK NOT FILMED

CONTENTS

ILLUSTRATIONS

INFRARED SPECTROSCOPY EXPERIMENT ON MARINER 9

PRELIMINARY RESULTS

The infrared spectroscopy experiment on Mariner 9 was designed to provide information on atmospheric and surface properties by recording a major portion of the thermal emission spectrum of Mars. The original intent was to derive vertical temperature profiles, surface temperature, atmospheric pressure at the surface, and information related to the surface composition. The experiment also was to search for minor atmospheric constituents, including water vapor and isotopic components of carbon dioxide (1). The biological implications of the Martian environment were to be studied. Although the Martian dust storm has complicated the task of attaining the scientific objectives originally formulated for a dust-free atmosphere, unexpected information on the dust composition and on the general circulation associated with the storm is being obtained.

The Michelson infrared interferometer spectrometer (IRIS-M) records the spectral interval from 200 cm^{-1} (50 μm) to about 2000 cm^{-1} (5 μm) with a nominal spectral resolution of 2.4 cm^{-1} in the apodized mode of data reduction. A noise equivalent radiance of about 5×10^{-8} W cm^{-2} $sterad^{-1}$ /cm^{-1} has been achieved. The field of view is almost circular with a half cone angle of 2.25°. Wavenumber calibration is provided by a fringe control interferometer that uses the 0.6929-μm line of a neon discharge source as a standard. Intensity calibration is achieved by scaling Mars spectra to calibration spectra recorded periodically while observing alternately deep space and a 296.4K on-board blackbody. After Fourier transformation and scaling of the raw spectra in an earth-based digital computer, the individual calibrated spectra are displayed in absoulte radiometric units as a function of wavenumber.

On a planetary scale, the Martian spectra obtained so far exhibit a fair degree of uniformity in comparison with similar spectra obtained from the Nimbus satellites for the earth (2). The major exception in the appearance of the Martian spectra occurs in the vicinity of the south polar cap. Examples of non-polar and polar spectra are shown in Figs. 1a and 1b, respectively.

Major features common to all spectra are the two broad regions at 400 to 600 cm^{-1} and 850 to 1250 cm^{-1} which appear in absorption in the non-polar spectra and in emission in the polar spectra and the molecular absorption by CO_2 in the range of 540 to 800 cm^{-1}. The difference in appearance of the spectra may be qualitatively ascribed to differences in the atmospheric temperature profile, the underlying lower boundary surface, and the amount of dust in the atmosphere. In most of the non-polar spectra, all of the molecular bands of CO_2 appear in absorption, indicating that the atmospheric temperatures decrease with height on a gross scale. In the polar spectrum, the parts of the spectrum from 550 to 625 cm^{-1} and 700 to 800 cm^{-1} appear in emission, indicating that the lower atmospheric regions in which this radiation originates is at a warmer temperature than the underlying surface.

The most striking result of the experiment thus far is the strong effect of the atmospheric dust on the emission spectra. The entire spectrum, with the exception of the strongly absorbing part of the 667 cm^{-1} (15 μm) CO_2 molecular band apparently is influenced to varying degrees by the opacity of the dust in the atmosphere. A rigorous treatment of spectra from a dust-laden atmosphere must be based on a radiative transfer model which incorporates absorption and scattering by the dust along with molecular CO_2 absorption. Until that can be accomplished, more simplified methods must suffice.

The diffuse features appearing near 470 and 1075 cm^{-1} in absorption in non-polar and emission in polar spectra are attributed to dust particles in the atmosphere. The features are characteristic of the $Si0_2$ bands in silicate-bearing minerals. Lyon (3, 4), Hovis (5), Aronson, et al. (6), Conel (7), and Salisbury, et al. (8) have shown that the spectral position of absorption and reflection peaks depends on the silica content; acidic minerals (70 to 75% $Si0_2$) suspended in powder form absorb most strongly at 1100 cm^{-1}, while ultra-basic materials (less than 45% $Si0_2$) show absorption peaks near 950 cm^{-1}. A preliminary comparison of the emission features measured over the south polar region with the absorption spectra of fine dust measured by Lyon shows generally good agreement with minerals and rocks whose $Si0_2$ content is in the intermediate range (55 to 65%), but poor agreement with highly acidic (greater than 65%), as well as basic (45 to 55%) and ultra-basic (less than 45%) material. Silicates are also indicated in non-polar areas. If this result is substantiated by continuing analysis (additional laboratory measurements of emission and absorption spectra of various dust samples, radiative transfer calculations for a scattering and absorbing atmosphere, analysis of additional spectra) its implications are of great planetological significance.

There is at this time no agreement on whether Mars is differentiated (see, e. g., 9, 10). The $Si0_2$ content of planetary surfaces is probably the best gross geochemical indicator of the degree of differentiation. Thus, the relatively high $Si0_2$ content indicated by these preliminary results, if representative of the Martian surface, would show that Mars has undergone at least as much differentiation as the moon (11), and perhaps as much as the earth. The above discussion assumes that the suspended dust has the same bulk composition as the surface rocks. This assumption is based on the probable absence of extensive chemical weathering on Mars.

The fact that the silicate features associated with the dust appear in emission in the polar spectra confirms that the absorption is produced by dust suspended in the atmosphere rather than the surface itself. The strength of the dust features in the spectra indicate a fairly substantial optical depth for the dust, especially in the regions away from the south polar cap or away from high plateaus.

Observation of the Martian surface has so far been possible only in the region of the south polar cap, and perhaps over highlands, where the atmospheric dust is sufficiently thin. For quantitative interpretation, it is first necessary to establish the radiance originating from the planetary surface. This, in general, depends on the emissivity of the surface material, the degree of homogeneity of the surface within the field of view in terms of temperature and composition, and the opacity of the dust-filled atmosphere. From a working model, a background radiance curve for the average south polar spectrum shown in Fig. 1b has been calculated and is included in the figure. The model assumes that an unknown fraction of the field of view is filled with a blackbody emitter at one temperature, while the rest of the field of view is filled with a blackbody at a second temperature. The model is based on the fact that the apparent size of the cap is slightly smaller than the IRIS field of view and is heterogeneous in structure. By using measured radiances at 295 cm^{-1}, 840 cm^{-1}, and 1330 cm^{-1}, and by assuming that they are unaffected by the atmosphere and by the dust in it, a fit was obtained with $65 \pm 5\%$ of the field containing an emitter at $140 \pm 10K$ and the remainder of the field filled with an emitter at $235 \pm 10K$. This result is consistent with a frozen CO_2 cap, in agreement with previous work (12, 13, 14).

Estimates of the vertical temperature structure of the atmosphere can be obtained from measurements in the 667 cm^{-1} CO_2 absorption band by inversion of the integral equation of radiative transfer. If the atmospheric transmittance is known, temperature as a function of atmospheric pressure level can be derived. Preliminary retrievals of temperature profiles have been made assuming an atmosphere consisting of 100% CO_2, and neglecting possible additional opacity due to dust. A knowledge of surface pressure is also required for an accurate specification of temperature in the lower atmospheric levels. The apparently near-isothermal structure of the lower atmosphere and the effects of dust opacity have prevented determination of surface pressure from the spectral data. Therefore, use has been made of surface pressure estimates from earth-based measurements and Mariner 6 and 7 data in regions where such data exist.

Examples of retrieved profiles are shown in Fig. 2. The profiles over Hellas and Sinai are typical of those obtained from spectra similar to the non-polar cases of Fig. 1a. Surface pressure was estimated for Hellas from Mariner 7 ultraviolet spectrometer measurements (15) and for Sinai from earth-based radar measurements (16) which were normalized at coincident points to Mariner 6 UVS pressure estimates. The lower lapse rates below 2-mb may be real. However, if the dust has approximately unity optical depth in the 15μm band at this level, a similar effect will result regardless of the true thermal structure in this region. Where the optical depth of the dust is less than unity, the temperature retrieval will be essentially unaffected by the presence of the dust. As the optical properties of the dust become better understood, the lower portion of the profiles, therefore, may be subject to revision. The temperatures above 2-mb are generally warmer than either those predicted theoretically for a dust-free atmsophere (17) or those obtained from the Mariner 6 and 7 occultation experiments (18, 19).

A profile obtained over the south polar cap is included in Fig. 2. Here, the most outstanding feature is the pronounced temperature inversion; this is responsible for the CO_2 bands being seen partly in emission as in the polar spectrum shown in Fig. 1b. Surface pressure estimates are not yet available in this region, but the basic behavior of the profile was essentially unaffected as the surface pressure was varied from 5 to 20 mb. Only the profile obtained using the 10-mb surface pressure is shown. Figure 3 shows isotherms for a vertical cross section along a single scan pass down onto the cap and back off of the cap again. The lower part of the diagram is uncertain because of the neglect of dust in the analysis and lack of knowledge of the surface pressure. The cross section shows a highly localized region of warm air at approximately 1 to 2 mb in the vicinity of the cap. The substantial solar illumination during the south polar summer, the reflection of solar energy by the cap, and atmospheric dynamical effects are all possible mechanisms for producing this effect.

The polar spectra also show rotational lines of water vapor in the region between 200 and 350 cm^{-1}. This portion of the IRIS spectrum from Fig. 1b has been expanded in Fig. 4. Consistent with atmospheric temperatures warmer than surface temperatures, the water vapor lines appear in emission. Also shown in Fig. 4 is a synthetic slant path spectrum composed using the two-surface temperature model described above. The excellent spectral correspondence verifies the existence of atmospheric water vapor in the south polar region. Water vapor spectral features appear more weakly over other regions of the planet. Possible reasons why water vapor is not more prominent there may be sought in the near-isothermal nature of the temperature profiles, the shielding effect of the dust, or possibly a lower water vapor concentration away from the south pole.

In summary, this experiment has been successful in providing information on the nature of the Martian atmosphere and surface. However, the conclusions appearing in this report must be regarded as preliminary. Further efforts will be devoted to a more rigorous analysis of the data. A search for minor constituents will be carried out on spectral averages using statistical techniques. Components of intrinsic biological interest will be sought. A better understanding of the optical properties of suspended dust requires laboratory transmission measurements as well as the development of applicable radiative transfer models. These models are expected to improve estimates of surface pressures, temperatures in the lower atmosphere, and the estimation of the amount of atmospheric water vapor. The results obtained by the infrared interferometer show the strength and versatility of high-resolution infrared spectroscopy as a tool for planetary exploration.

REFERENCES AND NOTES

1. R. A. Hanel, B. J. Conrath, W. A. Hovis, V. Kunde, P. D. Lowman, C. Prabhakara, B. Schlachman, and G. V. Levin, Icarus, 12, 48 (1970).

2. B. J. Conrath, R. A. Hanel, V. G. Kunde, and C. Prabhakara, J. Geophys Res., 75, 5831 (1970).

3. R. J. P. Lyon, Technical Note D-1871 (NASA, 1964).

4. R. J. P. Lyon, Contractor Report CR-100 (NASA, 1964).

5. W. A. Hovis, Appl. Opt., 5, 245 (1966).

6. J. R. Aronson, A. G. Emslie, R. V. Allen, and H. G. McLinden, J. Geophys. Res., 72, 687 (1967).

7. J. W. Salisbury, R. K. Vincent, L. M. Logan, and G. R. Hunt, J. Geophys. Res., 75, 2671 (1970).

8. J. E. Conel, J. Geophys. Res., 74, 1614 (1969).

9. T. C. Hanks, and D. L. Anderson, Phys. Earth Planet. Interiors, 2, 19 (1969).

10. A. E. Ringwood, and S. P. Clark, Nature, 234, 89 (1971).

11. P. D. Lowman, Jr., J. Geology (in preparation).

12. R. B. Leighton, and B. C. Murray, Science, 153, 136 (1966).

13. G. Neugebauer, G. Münch, H. Kieffer, S. C. Chase, and E. Miner, Astron. J., 76, 719 (1971).

14. K. C. Herr, and G. S. Pimentel in Mariner Mars 1969: A Preliminary Report (NASA, 1969), p. 83.

15. C. W. Hord, Icarus (in preparation).

16. G. H. Pettengill, A. E. E. Rogers, and I. I. Shapiro, Science (in preparation).

17. P. Gierasch, and R. Goody, Planet. Space Sci., 16, 615 (1968).

18. S. I. Rasool and R. W. Stewart, J. Atm. Sci., 28, 869 (1971).

19. A. J. Kliore, G. Fjeldbo, and B. L. Seidel, Space Research XI, (Adademie-Verlag, Berlin, 1971) p. 165.

20. The following people contributed substantially to the success of the IRIS experiment on Mariner 9: D. Crosby, R. Gerace, W. Maguire, W. Miller, L. Purves, and N. Spencer of Goddard Space Flight Center; T. Burke, H. Eyerly, and J. Taylor of the Jet Propulsion Laboratory; E. Breihan, R. Bywaters, D. Rodgers, D. Vanous, and L. Watson of Texas Instruments, Inc.; W. Andrews, R. Bevacqua, and R. Long of Consultants and Designers, Inc.; P. Straat of Biospherics Incorporated.

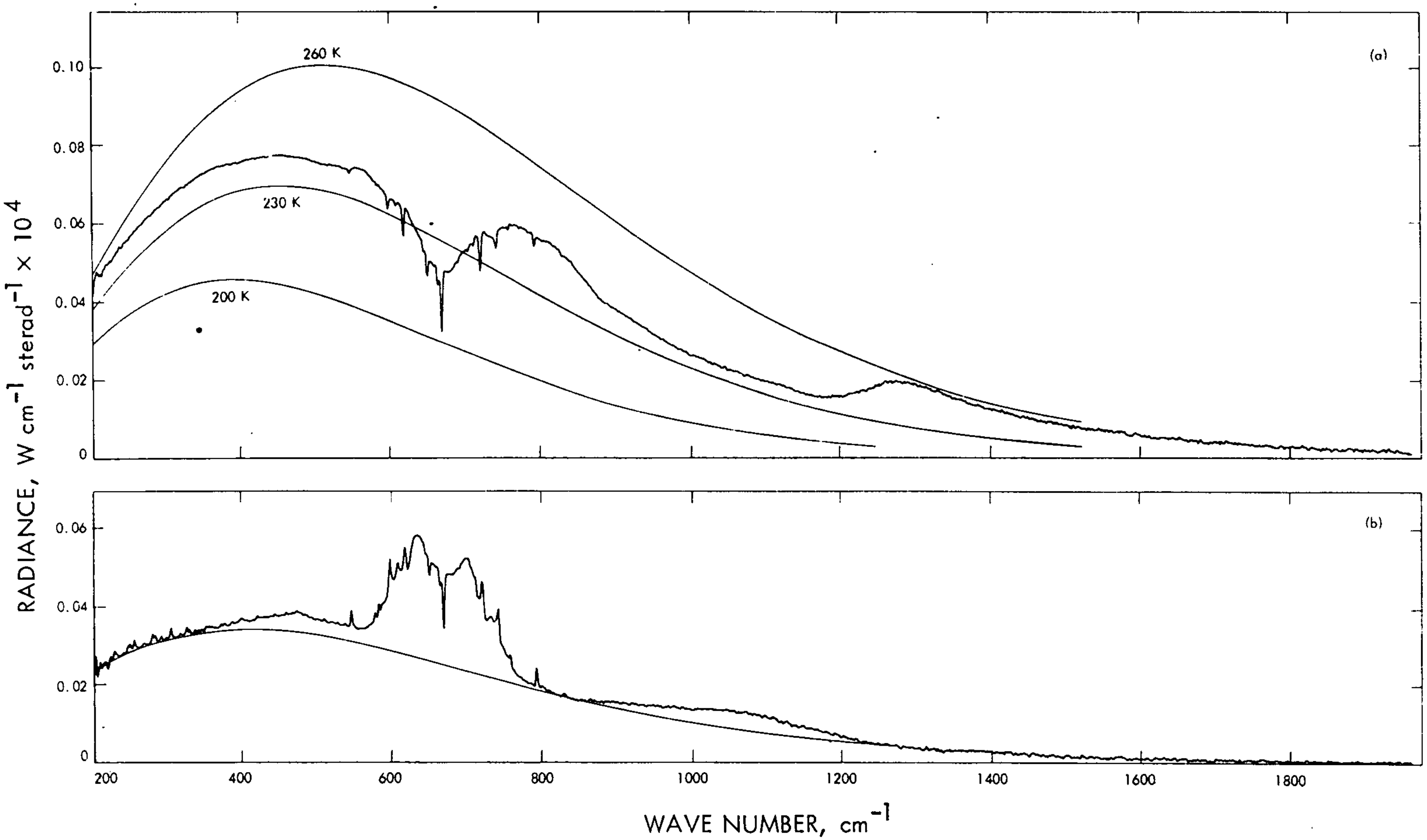

Figure 1. (a) Example of non-polar thermal emission spectra. The spectrum is the average of six spectra obtained from Rev 8 in the region of 18°S latitude and 13°W longitude at about 12:00 local time. Blackbody curves are included for comparison. (b) Example of polar thermal emission spectra with south polar cap in IRIS field of view. This spectrum is the average of six individual spectra obtained from Revs 29 and 30. The smooth curve is the composite of two blackbody spectra, as described in the text.

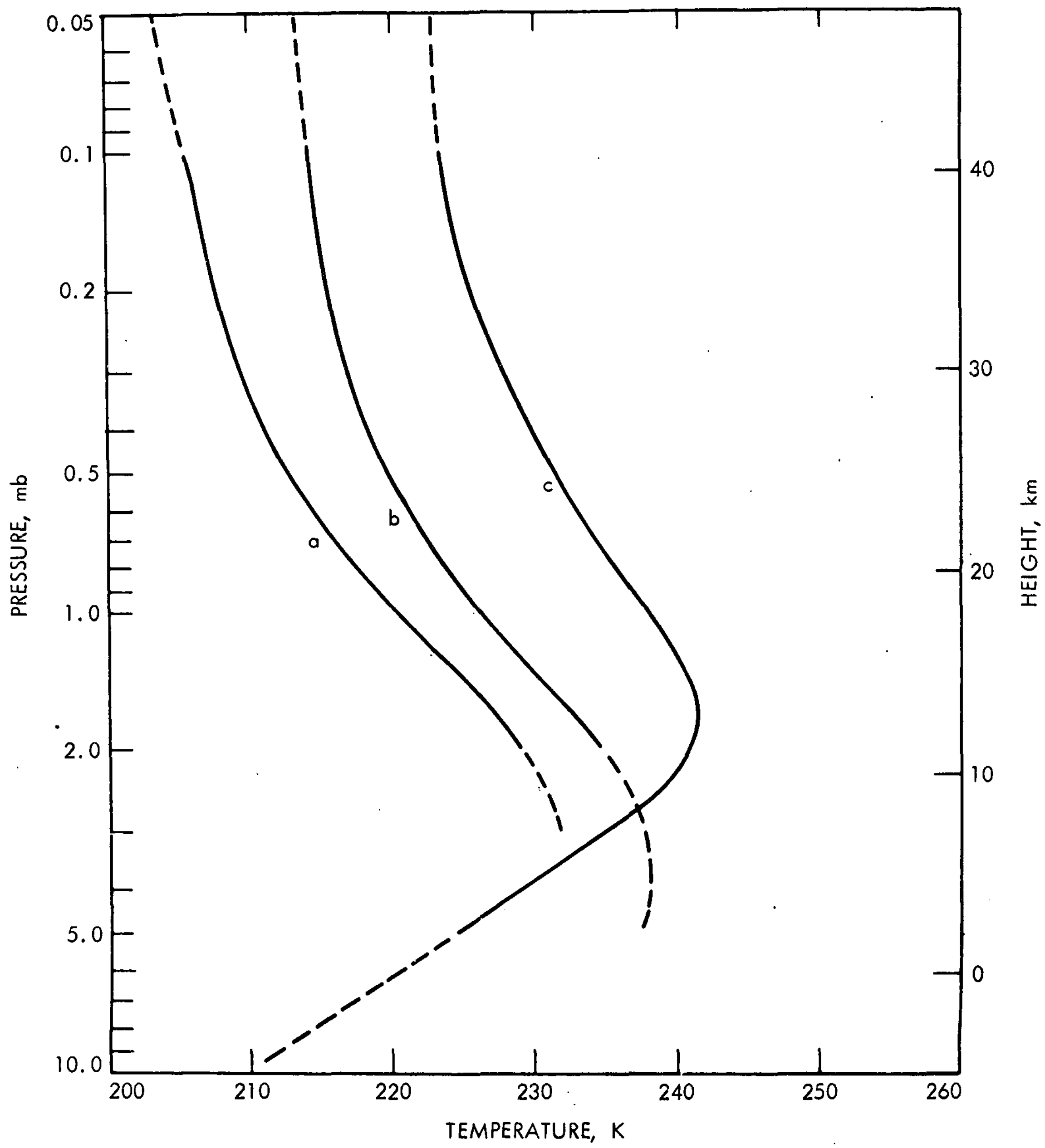

Figure 2. Temperature as a function of atmospheric pressure level for three Martian locations: 15.0°S, 64.2°W (Sinai) at 19:00 local time (a); 38.0°S, 282.8°W (Hellas) at 19:00 local time (b); 86.6°S, 342.2°W (south polar region) at 13:00 local time (c). The dashed parts of the curves are regarded as uncertain. An approximate height scale is included, using the triple-point pressure of water (6.1 mb) as a reference level.

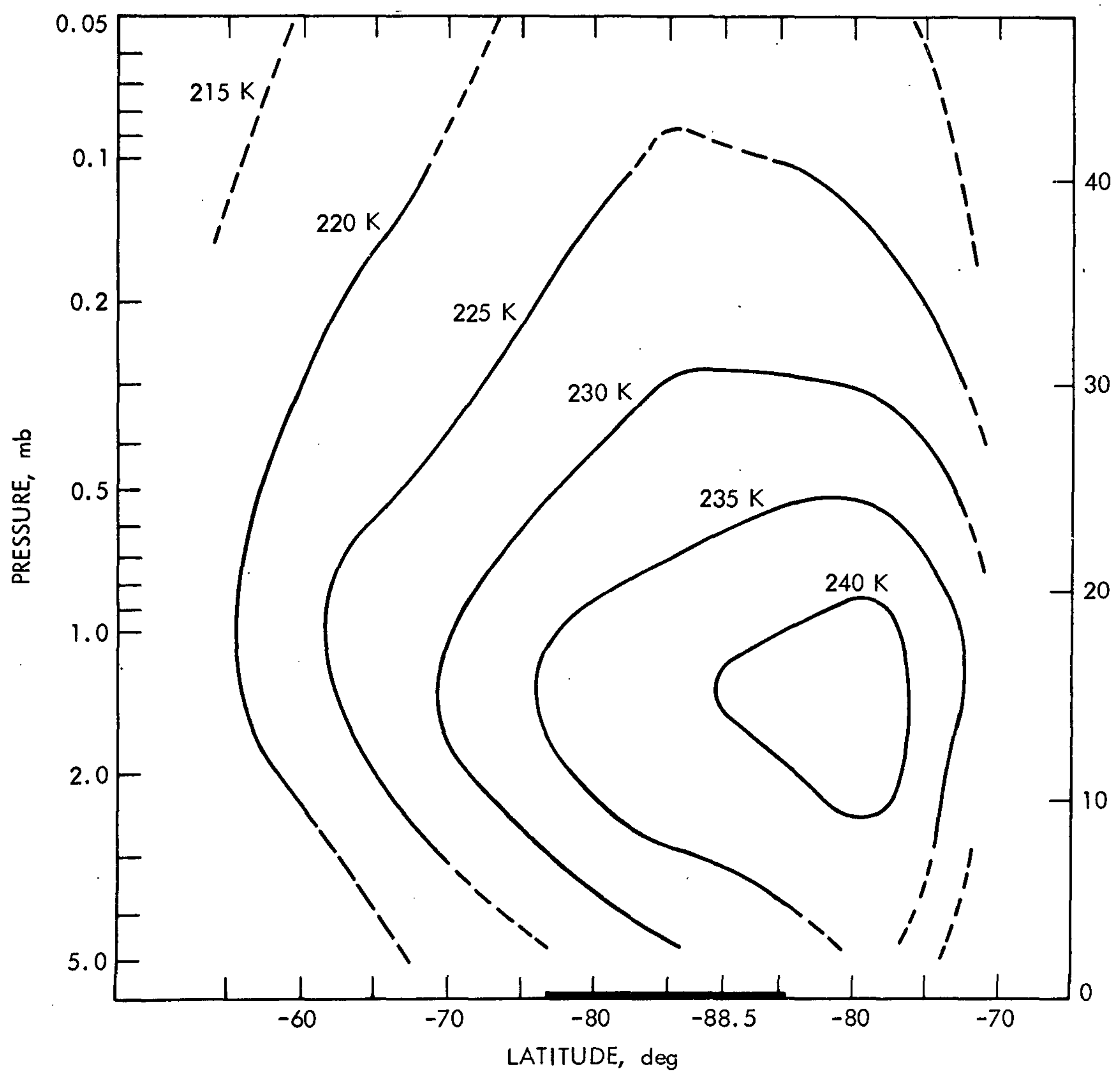

Figure 3. Isotherms for a cross section obtained from a single pass in the south polar region. The abscissa indicates the latitude of the center of the instrument's field of view as it approached the pole then moved away from it. Atmospheric pressure level is given along the ordinate with an approximate height scale similar to that of Fig. 2. Broken parts of the contours are uncertain. The heavy line at the bottom of the figure represents the extent of parts of the polar cap observed by the instrument.

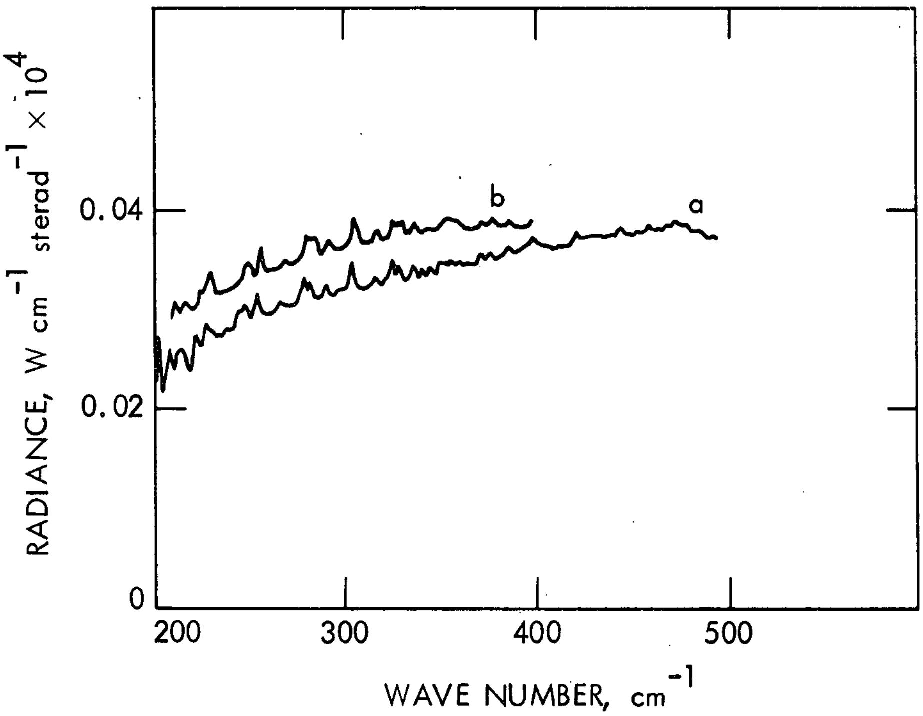

Figure 4. The 200 to 500 cm^{-1} portion of the south polar cap spectrum of Fig. 1b is shown on an expanded scale (a). The numerous spectral lines appearing in emission are due to rotational water vapor lines in the lower Martian atmosphere. A synthetic water vapor spectrum (b) is included for comparison; the spectrum has been shifted upward by 0.005 radiance units.